



HHS Public Access

Author manuscript

Acc Chem Res. Author manuscript; available in PMC 2019 May 02.

Published in final edited form as:

Acc Chem Res. 2019 March 19; 52(3): 802–817. doi:10.1021/acs.accounts.8b00663.

Soft Materials with Diverse Suprastructures via the Self-Assembly of Metal-organic Complexes

Yan Sun^{a,c,*}, Chongyi Chen^b, and Peter J. Stang^{c,*}

^aSchool of Chemistry and Chemical Engineering, Yangzhou University, Yangzhou, Jiangsu, 225002, P. R. China

^bNingbo Key Laboratory of Specialty Polymers, Ningbo University, Ningbo, Zhejiang 315211, PR China

^cDepartment of Chemistry, University of Utah, 315 South 1400 East, Room 2020, Salt Lake City, Utah 84112, United States

CONSPECTUS:

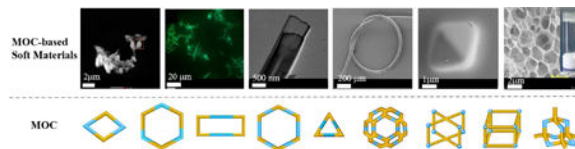
Inspired by assemblies in the natural world, researchers have prepared diverse suprastructures with distinct spatial arrangements by artificial self-assembly, including micelles, vesicles, ribbons, films, fibers, and tubes. The field of assembly is undergoing a transition from single-component to multicomponent assembly and single-step to multistep processing. Control over the size, shape, and composition of these building blocks has enabled the formation of suprastructures with substantial structural diversity. More importantly, harnessing noncovalent interactions to create suprastructures in a controlled manner will lead to a better understanding of the formation of complex self-organized patterns. However, for the construction of multiscale self-assemblies with controllable shapes and functions, the selection of a suitable protocol remains challenging.

Coordination-driven self-assembly provides a bottom-up approach to construct various metal-organic complexes (MOCs), which could be further used as building blocks with controllable shapes and sizes. Despite the tremendous progress made in the design of MOC-based supramolecular materials, most of these MOCs have dimensions of only several nanometers, and investigations of these structures rely on the characterization of their crystal structure. However, most of the functional suprastructures in living organisms have dimensions ranging from microns to centimeters and have the form of soft materials. Thus, obtaining MOC-based highly ordered materials of larger size remains a challenge.

This Account focuses on our recent advances in the construction of soft suprastructure materials with MOCs. A series of functionalized MOCs were first constructed through coordination-driven self-assembly. Then, further self-assembly of the as-prepared MOCs gave rise to the formation of higher-order structures. By changing the functional groups in the acceptors and donors in the MOCs, different suprastructures, including nanospheres, nanodiamonds, nanorods, nanofibers, membranes, films, and gels, were prepared. These studies suggest that using MOCs as building blocks is a highly efficient strategy to achieve complex architectures and functional materials for the development of desired MOC-based soft materials with high precision and fidelity.

*Corresponding Author sunyan@yzu.edu.cn, stang@chem.utah.edu.

Graphical Abstract



1. INTRODUCTION

Diverse suprastructures with distinct spatial arrangements can be obtained by artificial self-assembly. Currently, assembly is undergoing a transition from simple-component to multicomponent assembly and single-step to multistep processing. However, the selection of a suitable protocol for the construction of multiscale self-assemblies with controllable shapes and functions remains challenging. Coordination-driven self-assembly^{1–6} provides a powerful strategy for preparing molecules with well-defined sizes and shapes, which enables the transformation of different components into predesigned assemblies. Subsequently, the as-prepared assemblies could be further used as modular ‘building blocks’ for constructing higher-order superstructures with increasing complexity and functionality.

To date, a variety of different linking ligands have been used in controllable stoichiometries to furnish rhomboids,⁷ triangles,⁸ squares,⁹ hexagons,¹⁰ and polygons¹¹ with the aid of a metal acceptor having a 60°, 90°, 120°, or 180° angle. Furthermore, numerous functional units were incorporated as part of the dipyrindine/dicarboxylate donors. The introduction of alkyl chain segments into the precursors can result in the formation of amphiphilic metal-organic complexes (MOCs), which can subsequently hierarchically self-assemble into highly ordered nanostructures driven by hydrophobic effects. Rigid aromatic planar systems can provide π – π interactions,¹² amide or amino acid groups could provide hydrogen bonding sites,¹³ cholesteryl moieties feature van der Waals forces,¹⁴ and macromolecules¹⁵ can act as hosts by binding guest species. A hexagon can thus be assembled from the [6 + 6] combination of a linear ditopic organic donor and a binuclear metal acceptor with a 120° angle between metal sites or from the combination of a linear metal acceptor with a ditopic, 120° ligand. In addition to Pt, other metal ions, such as Pd,¹⁶ Cd,¹⁷ Ru,¹⁸ Au,¹⁹ Ag,²⁰ and Fe,²¹ can also be used, and their interactions with organic ligands lead to the formation of various MOCs. For example, van der Boom reported the synthesis of Cu(II)-based MOCs with TPEPA (1,3,5,7-tetrakis(4-(pyridyl-4'-yl-ethynyl)phenyl]adamantine) and Cu(NO₃)₂, and hollow tubes could be obtained by the further assembly of these MOCs.²² Regarding the acceptor, either nonfunctionalized di-Pt(II) acceptors with different binding angles or modified di-Pt(II) acceptors substituted with different functional groups can be chosen.

However, to date, studies have primarily focused on the relationship between metal acceptors and MOCs, whereas studies on the relation between MOCs and the resultant higher-order assemblies are rare. This has motivated us to systematically investigate the relationships among donor ligands, Pt acceptors, MOCs, and resultant assemblies. This review will further focus on the relationship between ligands and MOC-based higher order assemblies, as summarized in Scheme 1.

2. HIERARCHICAL SELF-ASSEMBLIES BASED ON PLATINUM-CONTAINING MOCs

2.1. Assembly of 60° organoplatinum (II) acceptor-based MOCs: Substituent effects (120° donors) on the higher-order assembly of rhomboids

Two 60° di-Pt(II) acceptors (**A60°**) and two 120° donors (**D**) were mixed to produce a rhomboid skeleton, (Figure 1a–c), and the rhomboidal MOCs (**M**) were obtained with various functional groups. Then, the Pt-based metal-organic rhomboids were used as building blocks to construct higher-order assemblies. Most of the rhomboids exhibited a tendency to form one-dimensional fibers. An amphiphilic rhomboid with a linear polyethylene glycol chain, **M1**⁷ (5.00×10^{-5} M), could self-assemble into fibers in water (Figure 1d). If the linear PEG group was replaced with branched PEG, **M2**⁷ could be prepared, and nanoribbons (Figure 1e) were obtained at the same concentration. Both **M1** and **M2** can form metallohydrogels. **M3** with long alkyl chains was prepared via a fragment coupling approach.²³ Upon exposure to a solvent mixture of dichloromethane/methanol, ordered fibers were formed (Figure 1f). The metallodendritic rhomboid **M4** could efficiently entrap solvent molecules to form a turbid gel (Figure 1g) in a mixed solvent of acetone and water with a very low critical gelation concentration (CGC) of $2.3 \text{ mg}\cdot\text{mL}^{-1}$.²⁴ The solvent ratio also plays an important role in tuning the morphologies of the resultant suprastructures. For the rhomboid cholesteryl-containing metallacycle **M5**, different morphologies, such as helical bundles and flowers (Figure 1h), were produced in mixed dichloromethane–methanol solvent systems with different solvent compositions at the same concentration of 0.2 mM.¹⁴ To investigate the influence of the chemical structure on aggregation behavior, analog **M6**, which contained amide groups as a linker, was also prepared.¹⁴ **M6** was found to form different macroscopic structures with different solvent compositions (dichloromethane/methanol), as shown in Figure 1i, well-dispersed nanoparticles were observed by the assembly of **M7** (0.1 mg/mL, 90% methanol).²⁵ However, when the concentration increased to 1.0 mg/mL, network structures were seen due to the further aggregation of the nanoparticles (Figure 1j). Decoration of the 60° organo-Pt(II) acceptors with Fréchet-type dendrons produced the rhomboidal metallodendrimer **M8**.²⁶ Upon the supramolecular polymerization of **M8** in CH_2Cl_2 , long, slightly bent nanofibers were subsequently found (Figure 1k).

2.2. Assembly of 90° organoplatinum (II) acceptor-based MOCs: Substituent effects on the higher-order assembly of metallacages

Eight 90° organoplatinum (II) acceptors (**A90°**), two faces (**F**) and four pillars (**P**) were mixed to produce metallacages (Figure 2a–d). By changing the substituents in the pillars, assemblies with various nanostructures were obtained. For example, tetra-(4-pyridylphenyl)ethylene (TPPE) could be used as a panel (Figure 2e), together with 90° organoplatinum (II) acceptors having dicarboxylate moieties (Figure 2f), to construct metallacage **M9**.¹² As shown in Figure 2g, microflowers were formed by the assembly of **M9** (10 μM) in a mixture of dichloromethane and ethyl acetate (80% ethyl acetate, EA). Anisotropic photoluminescence was observed when the microflowers were placed between

cross polarizers (inset). Autofluorescence was also observed in the microflowers. TEM images further demonstrated the formation of the microflowers.

A possible mechanism of microneedle formation (Figure 2h) involves the individual **M9** molecules dissolved in DCM and stacked via π - π interactions to form elongated one-dimensional (1D) supramolecular assemblies by the addition of EA, leading to the formation of microneedles. Subsequently, **M9**-based microflowers formed during solvent evaporation. Suprastructures with emissions ranging from blue and green to red were obtained through the coassembly of lysine-modified perylene (Figure 2i). Moreover, chlorophyll-a and Vitamin B₁₂ were introduced into the microflowers to construct a biomolecule-containing composite.

If a sodium sulfonate-modified dicarboxylate ligand was used as a pillar (Figure 2j) and interacted with TPPE and the 90° acceptor, **M10** was obtained. In water, **M10** (25 μ M) self-assembled into microfibers (Figure 2k).²⁷ At the same concentration, microspheres formed by **M10** in tetrahydrofuran (Figure 2l). If a nitro group-modified dicarboxylate ligand was used as a pillar (Figure 2m) and interacted with the same face and acceptor, **M11** was obtained. At the same concentration (25 μ M), **M11** further assembled into microplates in tetrahydrofuran (Figure 2n). Whereas a microfilm formed by the assembly of **M11** in ethanol (Figure 2o).²⁷ If a methoxy group-modified dicarboxylate ligand was used as a pillar (Figure 2p), **M12** was obtained. In tetrahydrofuran, **M12** (25 μ M) self-assembled into hollow spheres (Figure 2q). If an amine group-modified dicarboxylate ligand was used as a pillar (Figure 2r), **M13** was obtained. In tetrahydrofuran, **M13** (25 μ M) self-assembled into microsheets (Figure 2s).²⁷ Metallacages were prepared by the assembly of tetraphenylethylene (TPE)-based sodium benzoate (Figure 3a), a pillar (Figure 3b), and a 90° acceptor. Stang et al. prepared a multifunctional **M14**-based supramolecular gel by orthogonal metal coordination and host-guest interactions (Figure 3c-e).¹⁵ In addition to TPE-containing metallacages, porphyrin-based metallacages were used as building blocks to construct MOC-based materials. Huang et al. prepared porphyrin metallacage **M15** (Figure 3f-g) and then studied the host-guest complexation between **M15** and pyrene (Figure 3h). It was found that a liquid-crystalline complex was formed (Figure 3i).²⁸

2.3. Assembly of 120° organoplatinum (II) acceptor-based MOCs: Substituent effects on the assembly of hexagons

Three 120° organoplatinum (II) acceptors (**A120°**) and three 120° donors were mixed to produce hexagon MOCs (Figure 4a-c). Hexagons **M16-20** were decorated with various functional groups by using **A120°-1** (Figure 4d) and different donors **D9-13**. Yang et al. designed and synthesized 120° dipyriddy donors (e.g., **D9**) functionalized with multiple amide groups and long hydrophobic alkyl chains (Figure 4e) to produce discrete hexagonal metallacycles (**M16**), that could form a supramolecular polymeric hydrogel, promoted by CO₂, near physiological temperature (Figure 4e, SEM).²⁹ Yang et al. also reported the successful combination of coordination-driven self-assembly and post-assembly reversible addition fragmentation chain-transfer polymerization to produce a new family of star supramolecular polymers containing well-defined metallacycles (**M17**).³⁰ Aqueous solutions of **M17** formed free-standing macroscopic hydrogels at room temperature in only 5 min.

The critical gelation concentrations (CGCs) were determined to be 2.5 wt % (Figure 4f, SEM). When a very dilute solution of the mixture of tris-TPE metallacycle **M18** and heparin was dropped on a freshly cleaved mica surface, some single bead-like chains were observed (Figure 4g).³¹ Esterification of 3,5-bis(pyridin-4-ylethynyl) phenol (BisPy-OH) with N-[2-(3,4,5-tridodecylcyclo-xylbenzoylamino)ethyl succinic acid (G12-en-SA acid) yielded the desired 120° dipyriddy donor (**D12**). Then, the self-assembly of [3+3] metallacyclic hexagon **M19** was investigated. **M19** formed an almost uniform and highly ordered fibrous network structure upon exposure to a mixed solvent of acetone and water at a low concentration (5.0×10^{-2} mM). The width of these fibers is within the range of 100–200 nm, and each fiber is a few micrometers in length (Figure 4h, SEM).³² Yang et al. designed and constructed peripherally DMIP-functionalized poly(benzyl ether) metallodendrimer **M20**.³³ The dendritic hexagon **M20** assembled into vesicular structures (Figure 4i, SEM) in a mixed solvent of acetone and tetrahydrofuran. In addition to the influence of the substituents in the donor on the resultant assemblies, the acceptor was also modified with a functional group (Figure 5a).

A TPE-based supra-amphiphilic metallacycle was functionalized with three poly (N-isopropylacrylamide) arms through a combination of an exo-functionalization strategy and post-assembly polymerization. An aqueous solution of **M21** with a concentration of 1.0 mg mL⁻¹ was deposited on copper grids, and nanoparticles with a size distribution of approximately 20 nm were observed (Figure 5b–d).³⁴ Furthermore, Yang et al. reported the successful preparation of structurally defined porous membranes based on hexakistriphenylamine metallacycle **M22** through electropolymerization (Figure 5e–g).³⁵ A discrete hexagonal metallacycle **M23** decorated with TPE, amide groups and long hydrophobic alkyl chains was constructed via [3 + 3] coordination-driven self-assembly. **M23** formed organometallic gels (Figure 5h–j) in acetone/water at a low CGCs (21.3 mg.mL⁻¹).³⁶ A complementary organoplatinum (II) acceptor (Figure 5k) having a crown ether moiety and a UPy-functionalized rigid dipyriddy donor (Figure 5l) were used to construct **M24**, which forms a gel-like soft material at high concentrations or upon solvent swelling (Figure 5m).³⁷ Huang et al. also prepared a organoplatinum acceptor (Figure 5n) that underwent coordination-driven self-assembly with a complementary highly directional dipyriddy donor functionalized with a benzo-21-crown-7 moiety (Figure 5o) to furnish hexagonal metallacycle **M25**. These hexagons subsequently polymerize into a supramolecular network upon the addition of a bisammonium salt due to the formation of pseudorotaxane linkages between the crown ether and ammonium moieties. At high concentrations, the resulting assemblies become a gel comprising many cross-linked metallohexagons (Figure 5p).³⁸ With the TPE-based metallacycle **M26** used as a positively charged molecular “glue”, the rod-like tobacco mosaic virus (TMV) with a negatively charged surface can be assembled into three-dimensional (3D) micrometer-sized bundle-like superstructures via multiple electrostatic interactions (Figure 5q–s).³⁹

2.4. Assembly of 180° organoplatinum (II) acceptor-based MOCs: Geometry effects of MOCs on higher-order assembly

Additional polygons were obtained via the use of 180° acceptors (**A180°**), including triangles, diamonds, and rosettes. For example, Yang and coworkers designed and

synthesized a dipyridyl donor containing a central Z-configured stiff-stilbene unit that self-assembles in the presence of two 180° di-Pt(II) acceptors, **A180o-1** and **A180o-2** (Figure 6a), to produce size-controllable organoplatinum(II) metallacycles **M27–28** (Figure 6b).

These metallacycles aggregated into spherical nanoparticles that evolved into long nanofibers upon polymer formation. These fibers were reversibly converted to cyclic oligomers by changing the wavelength of irradiation (Figure 6c–d).⁹ Yang et al. reported the construction of hexakispillar[5]arene metallacycles via coordination-driven self-assembly. A 120° pillar[5]arene containing a dipyridyl donor (Figure 6f) was combined with the corresponding complementary 180° di-Pt(II) acceptors with different lengths (**A180o-1** and **A180o-2**). Crosslinked supramolecular polymers were constructed from the hexakispillar[5]arene metallacycles **M29, 30**, (Figure 6g–h).¹⁰ Yang et al. also designed and constructed dendritic dipyridyl donors (Figure 6i), from which two novel triangular metallodendrimers, **M31, 32**, were successfully prepared. This generated dendron was found to significantly influence the hierarchical self-assembly behaviors of triangular metallodendrimers (Figure 6i–l)⁸, which were further used as building blocks to construct nanoparticles and nanofibers. Then, they synthesized **M33, 34** (Figure 6m) and prepared **M33, 34**-based gels (Figure 6n–o).¹¹ In addition to nanofibers, nanospheres, and gels, nanodiamonds were prepared by a stepwise assembly through the combination of 120° and 180° diplatinum(II) acceptors. Cao combined the concepts of supramolecular coordination complexes and metal-organic frameworks to offer a new strategy for constructing a diamondoid supramolecular coordination framework from an adamantanoid supramolecular coordination cage as the tetrahedral node and a difunctional Pt(II) ligand as a linear linker via the stepwise orientation-induced supramolecular coordination, producing **M35** (Figure 6p–r). SEM images obtained from a solution of **M35** in DMSO upon solvent evaporation at 50°C showed that nanometer-sized structures self-assembled into a micrometer-sized regular octahedron with a side length of ~2.12 μm and a calculated volume of ~4.49 μm³ (Figure 6s).⁴⁰

2.5. Substituents effect and geometry effects on the higher-order assembly of MOCs

As mentioned above, both functional groups and the geometry of the MOC are important for tuning the higher-order assembly. These effects were elucidated by using the same donors but different acceptors (Figure 7a–f) to construct MOCs with different shapes (Figure 7g). In some cases, substituents and not the geometry of the MOCs play an essential role in controlling the morphology. In particular, some directional groups, such as hydrogen bonding containing groups, act as functional groups. For example, Sun and coworkers reported the design and synthesis of alanine-based chiral precursor **D26** (Figure 7h), which is amenable to coordination-driven self-assembly and forms chiral organoplatinum(II) metallacycle rhomboids **M36, 37** and hexagons **M38, 39**.¹³ Gels with higher-order self-assembled nanostructures were formed by subsequent hydrogen bonding interactions. The morphologies of metallogels **M36, 37** and **M38, 39** at their critical metallogelation concentrations were explored by SEM and TEM, which revealed that all assemblies formed interconnected fibers (Figure 7i–l) with well-defined helicity.¹³

Stirring a mixture of **D27** (Figure 7m) and 60° organoplatinum(II) acceptor 3,6-bis[trans-Pt(PEt₃)₂(NO₃)₂]phenanthrene **A600-1** (Figure 7a) in CD₃OD induced the self-assembly of [2 + 2] rhomboid **M40** functionalized with 2-ureido-4-pyrimidinone at its vertices. Self-assembled [3 + 3] hexagons were prepared in a similar fashion by mixing **D27** with one of two 120° organoplatinum(II) acceptors, 1,3- bis[trans-Pt(PEt₃)₂(OTf)₂ ethynyl]benzene (**A1200-6**, forming hexagon **M41** or 4,4'-[trans-Pt(PEt₃)₂(NO₃)₂]diphenyl ketone (**A1200-1**, forming hexagon **M42**), in DMSO for 8 h. The TEM image in Figure 7n shows a rod-like fiber made by placing one drop of dichloromethane solution of rhomboid **M40** (1.00 mM) onto a carbon-coated copper grid. SEM images show that a thin-long fiber could be drawn from the swelled UPy-functionalized hexagon **M41** (Figure 7o) and that a knotted fiber could be formed from solvent-swelled UPy-functionalized hexagon **M42** (Figure 7p).⁴¹

In some cases, the geometry of the MOC and not the substituents plays an important role in controlling the morphology of the resultant assemblies. In these cases, the donors contained only alkyl chains and not amide groups. Yang et al. reported the preparation and characterization of a family of metallacycles with different shapes and sizes along with long alkyl chains (Figure 7q). Due to the different geometrical properties and alkyl chain densities, the resulting metallacycles exhibited distinct self-organization patterns on different surfaces, Si(111) or mica, thus yielding various nanostructures with ordered sizes and shapes. For instance, rhomboidal complex **M43** resulted in a fibrous morphology on the surface (Figure 7r), whereas hexagonal complexes **M44** and **M45** generated nanospheres under the same conditions (Figure 7s–t).⁴⁴ They also reported the successful construction of alkynylplatinum(II) bzimpy-functionalized hexagonal metallacycle **M46** by coordination-driven self-assembly of **D29** (Figure 7u) and acceptors. **M46** was able to hierarchically self-assemble into a stable supra-molecular metallogel (Figure 7v) at room temperature. Further investigation revealed that this metallogel was selectively responsive to coronene as an aromatic guest, which induced the gel-to-sol transition by disrupting intermolecular Pt···Pt and π–π stacking interactions.⁴³ However, the rhomboids could not form a stable gel, possibly due to the weak intermolecular interaction of the rhomboids.

Furthermore, Yang and coworkers synthesized 120° triphenylamine-substituted dicarboxylate donor ligands **D30** (Figure 7w) and complementary 120° TPA-functionalized di-Pt(II) acceptor building blocks. Then, metallacycles (**M47**, **48**) with different shapes and sizes were successfully obtained *via* the formation of oxygen-to-platinum coordination bonds. Subsequently, post-electropolymerization of those two neutral multi-TPA-containing metallacycles resulted in the fabrication of a new type of neutral polymeric film with well-controlled cavity sizes and thickness. As shown by TEM, the **M47** film displayed a sheet-like morphology (Figure 7x) rather than the linear fiber observed for **M48** (Figure 7y).⁴⁴

5. Palladium-containing MOCs and the resultant soft materials

In addition to platinum, Pd has also been used as a building block to construct higher-order assemblies. Johnson et al. synthesized the star polymer MOC material M₁₂L₂₄ (**M49**) (Figure 8a), which can be used to precisely tune the structure and dynamics of polymer networks (Figure 8b).⁴⁵ Then, they reported gels assembled from polymeric ligands and MOCs as junctions. The resulting ‘polyMOC’ gels are precisely tunable and may feature

increased branch functionality. They show two examples of such polyMOCs: a gel based on an M_2L_4 paddlewheel cluster junction, **M50**, and a compositionally isomeric one based on an $M_{12}L_{24}$ cage (**M51**, Figure 8c–e).¹⁶ Fujita et al. constructed well-defined $M_{12}L_{24}$ **M52** spherical frameworks containing 24 forklike mesogens on the surface of the spheres. They also produced spherical complexes/polymer hybrid LC nanostructured gels that exhibit self-healing properties through the formation of dynamic covalent bonds (Figure 8f).⁴⁶ Shionoya et al. prepared macrocyclic skeletons of ligand 1 and found that its Pd(II) complexes **M53**, **54** allowed their stacked arrangement to form 1D organic and organometallic fibrous aggregates (Figure 8g).⁴⁷ Huang et al. designed and synthesized a Pd_2L_4 metallacage **M55** with four appendant pillar[5]arene units (Figure 8h) and a neutral ditopic guest compound. A supramolecular polymer gel prepared by self-assembly showed temperature and H^+ responsiveness due to the dynamic metal coordination and host–guest interactions, making the supramolecular gel act as a smart material (Figure 8i).⁴⁸

6. Au/Ag/Fe/Co/Ru/Cd-containing MOCs

The Aida group reported that a trinuclear Au(I) pyrazolate complex (**M56**) bearing long alkyl chains (Figure 9a) in hexane self-assembled via a Au(I)–Au(I) metallophilic interaction to form a red-luminescent organogel (Figure 9b).¹⁹ The Gao group reported that a heterochiral metallocycle **M57** (Figure 9c) was formed by the self-discriminating assembly of racemic bisbipyridines and silver ions and was further self-organized into nanofibers immobilizing self-assembled metal–organic cages.²⁰ These materials selectively encapsulated organic solvents in a distinct pattern from the enantiopure version (Figure 9d). The Nitschke group reported a new class of hydrogels formed by polymers that are cross-linked through subcomponent guest molecules within the cages. **M58** (Figure 9e, left) forms two distinct internal phases within the hydrogel, which allows contrasting release profiles of related molecules depending on their aptitude for encapsulation within the cages (Figure 9e, right).²¹

The Newkome group characterized a unique pentameric metallomacrocyclic, **M59**, as well as its predesigned hexameric cousin (**M60**), from the Fe(II)-mediated complexation of functionalized 3,5-bis(terpyridinyl)arene ligands (Figure 9f). The self-assembled nanofibers based on **M59** and **M60** were generated by slowly diffusing hexane into macrocycle solutions ($3 \text{ mg}\cdot\text{mL}^{-1}$) in a mixed solvent (Figure 9g).⁴⁹ The Izzet group reported the preparation of multiscale nanoarchitectures **M61**, **62** (Figure 9h–i) through metal-driven self-assembly processes. They found that the solvent composition and the charge of the metal linker are key parameters that steer the supramolecular organization. Different types of hierarchical self-assemblies, namely, zero-dimensional dense nanoparticles and 1D worm-like nano-objects, were selectively formed due to the different aggregation modes of the metallomacrocycles (Figure 9j).⁵⁰ The Newkome group also reported the self-assembly of multi-ionic species through electrostatic interactions for rigid polycationic macrocycles **M63** with spherical polyanionic dendrimers. The hierarchical formation of the nanofibers and sphere-like clusters has demonstrated the potential to employ polyionic architectures as aids in shape control (Figure 9k).¹⁸ Li et al. used the complete conjugate of TPE with 2,2':6',2''-terpyridine (TPY) as a ligand assembled with Cd(II) to immobilize fluorophores into rosette-

like metallo-supramolecules **M64–65** (Figure 9l–m), which were used as building blocks for fabricating nanotubes with different diameters (Figure 9n–o).¹⁷

6. Possible mechanism of Pt containing MOCs based higher-order soft materials

As describe above, various MOCs have been used for constructing higher-order soft materials (Figure 10a), in particular, two dimensional MOCs such as hexagons and rhomboids have been widely investigated. As shown in Figure 10b, 48% of the soft materials were constructed with hexagons, and 27% were constructed with rhomboids. Based on these data, we try to provide the mechanism of the formation higher-order soft materials. For example as seen in Figure 10c, 54% of the soft materials are fibers or rods which grow in one dimension. These MOC rhomboids were composed of multiple benzene rings, which suggests that $\pi - \pi$ interactions plays the dominant role in the formation of the resultant materials, and thereby providing the driving force for the stacking of rhomboids along a one dimensional direction. However, functional groups also play an important role in tuning the morphology. Rhomboids with hydrogen bonding donor/acceptor sites drive and stabilize the formation of one-dimensional structure (**M 3, 4, 8, 36, 37**). As for the hexagons based soft materials, more than half of them (57%) are gels, and 17% of the materials are one-dimensional fibers (Figure 10d). Unlike the more rigid planer skeleton of rhomboids, hexagons are more flexible and less planar, and therefore harder to grow in only one direction. As a result, gels instead of fibers become the dominant structure during higher-order assembly. Compared with two-dimensional MOCs, the further assembly of three-dimensional metallacages into higher-order systems is still in the initial stage. In order to minimize the influence of substituents, the parent metallacages are used to illustrate the mechanism. The formation of microneedles demonstrate the importance of aromatic interaction in tuning the assemblies' morphology. For metallacages with aromatic groups in three dimensions, it is not possible to form simple one dimensional architectures. Thus, the driving force of the formation of microflowers might result from the aromatic interaction among microneedles, which is similar to the formation of the hexagon based gel. Furthermore, concentrations of MOCs, environmental temperature, solvent ratio etc are all important factors in tuning the assemblies' morphology. However, based on the limited data, to date the comprehension of the accurate relationships among concentrations, temperature, solvent ratio, and other metal containing MOCs are far from understood.

6. CONCLUSION AND PERSPECTIVES

Self-assembly is the spontaneous organization of multiple components into well-defined ensembles based upon the recognition elements embedded in the building units. Nature has evolved self-assembly to readily form complex molecules, aggregation and other entities essential for life. Nature is the master of self-assembly by ingeniously exploiting a multitude of weak, noncovalent interactions, such as hydrogen bonding, $\pi - \pi$ stacking, dipole-dipole, van der Waals, hydrophobic-hydrophilic, to enable countless biological processes. Inter alia, nucleic acid structures, proteins folding, ribosomes, chromosomes, membranes, microtubules are examples of self-assembly of critical importance in all living organisms. In

the last couple of dozen years abiological self-assembly has emerged as a cutting edge, major and active area of the chemical sciences. As described in this Account abiological self-assembly using metal-organic complexes based upon metal-ligand interactions by itself or in combination with other weak interactions has provided a convenient procedure for the formation of countless novel soft materials with diverse morphologies and properties. Using this approach different suprastructures, such as nanorods, nanofibers, nanospheres, diamond like architectures as well as films and porous gels have recently been prepared, characterized and investigated. Yet this is just the beginning of the journey to prepare ever more sophisticated and complex ensemble for application in the materials, biochemical, biomedical as well as other areas. Furthermore, many challenges remain in this field. The self-assembly process itself is far from fully understood. The precise relationship between the metal ligand structure, MOC's and the resultant suprastructure needs to be explored. The use of metals, other than mostly Pt and Pd, and simple synthesis of needed organic ligands must be further developed. Finally and perhaps most importantly chemists should interact and collaborate more with other scientists like biologists, physicists, engineers and medical doctors to take full advantage of the power of abiological self-assembly to the benefit of human health and wellbeing.

Funding

National Natural Science Foundation of China (21503185 and 21404062)

NIH (Grant R01-CA215157)

NSF (CHE-1506722)

NIH (1R01GM128037-01)

Biographical Information

Yan Sun obtained her Ph.D. degree at the Institute of Chemistry, Chinese Academy of Sciences, in Beijing in 2012. Her research interests mainly focus on the synthesis of functional molecules and assembly based on these molecules. She joined the faculty at Yangzhou University, China, as an Assistant Professor in 2014. She joined Professor Peter J. Stang's group at University of Utah in 2017, and now she is investigating metal-organic complexes (MOCs) and MOC-based assembly.

Chongyi Chen obtained his Ph.D. degree in 2013 from the Institute of Chemistry, Chinese Academy of Sciences, and Peking University. He joined the faculty at Ningbo University, China in 2013 and is an Assistant Professor in the Department of Polymers at Ningbo University. His research interests include polypeptide-based chemistry and materials.

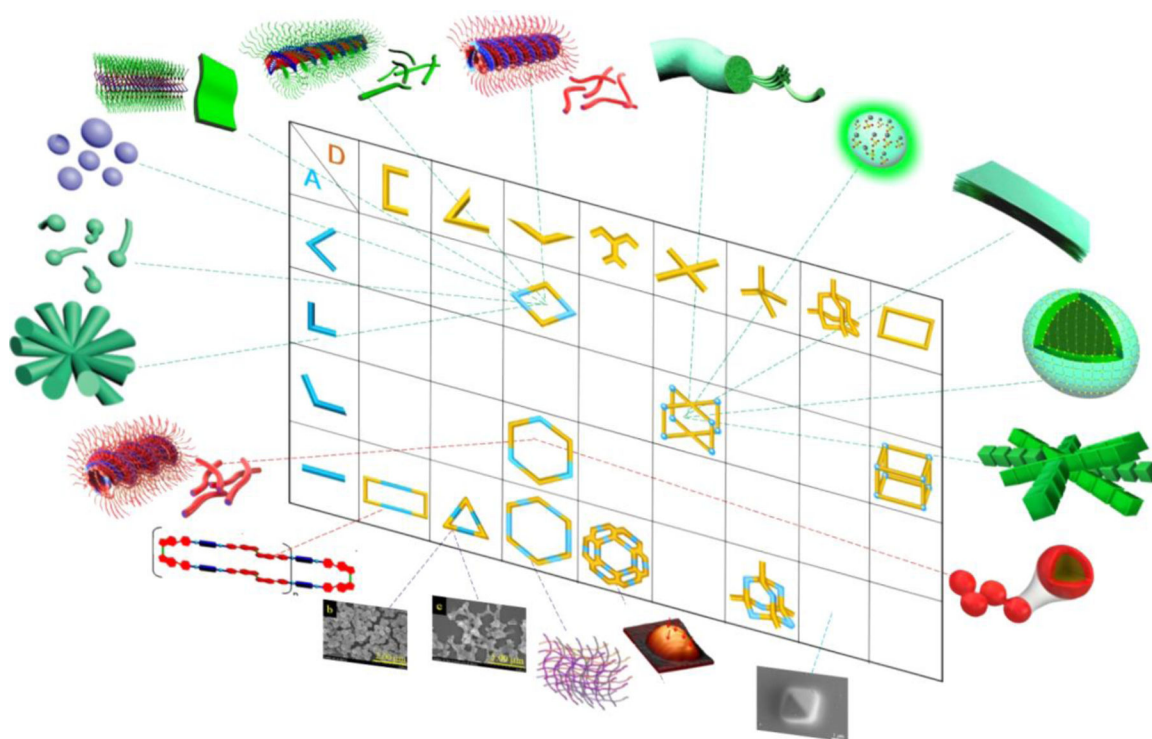
Peter J. Stang is the David P. Gardner distinguished professor of Chemistry. He is a member of the US National Academy of Sciences, a foreign member of the Chinese Academy of Sciences, and the recipient of the Chinese Government "International Cooperation Award in Science and Technology" (2016), the ACS Priestley Medal (2013), and the US National Medal of Science (2011).

References

- (1). Clever GH; Punt P Cation–Anion Arrangement Patterns in Self-Assembled Pd₂L₄ and Pd₄L₈ Coordination Cages. *Acc. Chem. Res* 2017, 50 (9), 2233–2243. [PubMed: 28817257]
- (2). Saha ML; Yan X; Stang PJ Photophysical Properties of Organoplatinum(II) Compounds and Derived Self-Assembled Metallacycles and Metallacages: Fluorescence and its Applications. *Acc. Chem. Res* 2016, 49 (11), 2527–2539. [PubMed: 27736060]
- (3). Chakrabarty R; Mukherjee PS; Stang PJ Supramolecular Coordination: Self-Assembly of Finite Two- and Three-Dimensional Ensembles. *Chem. Rev* 2011, 111 (11), 6810–6918. [PubMed: 21863792]
- (4). McConnell AJ; Wood CS; Neelakandan PP; Nitschke JR Stimuli-Responsive Metal–Ligand Assemblies. *Chem. Rev* 2015, 115 (15), 7729–7793. [PubMed: 25880789]
- (5). Newkome GR; Moorefield CN From 1 → 3 dendritic designs to fractal supramacromolecular constructs: understanding the pathway to the Sierpiński gasket. *Chem. Soc. Rev* 2015, 44 (12), 3954–3967. [PubMed: 25316287]
- (6). Wang W; Wang Y-X; Yang H-B Supramolecular transformations within discrete coordination-driven supramolecular architectures. *Chem. Soc. Rev* 2016, 45 (9), 2656–2693. [PubMed: 27009833]
- (7). Yan X; Li S; Cook TR; Ji X; Yao Y; Pollock JB; Shi Y; Yu G; Li J; Huang F; Stang PJ Hierarchical Self-Assembly: Well-Defined Supramolecular Nanostructures and Metallohydrogels via Amphiphilic Discrete Organoplatinum(II) Metallacycles. *J. Am. Chem. Soc* 2013, 135 (38), 14036–14039. [PubMed: 23927740]
- (8). Jiang B; Chen L-J; Zhang Y; Tan H-W; Xu L; Yang H-B Hierarchical self-assembly of triangular metal dendrimers into the ordered nanostructures. *Chin. Chem. Lett* 2016, 27 (4), 607–612.
- (9). Yan X; Xu J-F; Cook TR; Huang F; Yang Q-Z; Tung C-H; Stang PJ Photoinduced transformations of stiff-stilbene-based discrete metallacycles to metallosupramolecular polymers. *Proc. Natl. Acad. Sci* 2014, 111 (24), 8717–8722. [PubMed: 24889610]
- (10). Li Z-Y; Zhang Y; Zhang C-W; Chen L-J; Wang C; Tan H; Yu Y; Li X; Yang H-B Cross-Linked Supramolecular Polymer Gels Constructed from Discrete Multipillar[5]arene Metallacycles and Their Multiple Stimuli-Responsive Behavior. *J. Am. Chem. Soc* 2014, 136 (24), 8577–8589. [PubMed: 24571308]
- (11). Sun B; Wang M; Lou Z; Huang M; Xu C; Li X; Chen L-J; Yu Y; Davis GL; Xu B; Yang H-B; Li X From Ring-in-Ring to Sphere-in-Sphere: Self-Assembly of Discrete 2D and 3D Architectures with Increasing Stability. *J. Am. Chem. Soc* 2015, 137 (4), 1556–1564. [PubMed: 25574776]
- (12). Sun Y; Zhang F; Jiang S; Wang Z; Ni R; Wang H; Zhou W; Li X; Stang PJ Assembly of Metallacages into Soft Suprastructures with Dimensions of up to Micrometers and the Formation of Composite Materials. *J. Am. Chem. Soc* 2018, 140 (49), 17297–17307. [PubMed: 30424604]
- (13). Sun Y; Li S; Zhou Z; Saha ML; Datta S; Zhang M; Yan X; Tian D; Wang H; Wang L; Li X; Liu M; Li H; Stang PJ Alanine-Based Chiral Metallogels via Supramolecular Coordination Complex Platforms: Metallogelation Induced Chirality Transfer. *J. Am. Chem. Soc* 2018, 140 (9), 3257–3263. [PubMed: 29290113]
- (14). Chen L-J; Jiang B; Yang H-B Transformable nanostructures of cholesteryl-containing rhomboidal metallacycles through hierarchical self-assembly. *Org. Chem. Front* 2016, 3 (5), 579–587.
- (15). Lu C; Zhang M; Tang D; Yan X; Zhang Z; Zhou Z; Song B; Wang H; Li X; Yin S; Sepehrpour H; Stang PJ Fluorescent Metallacage-Core Supramolecular Polymer Gel Formed by Orthogonal Metal Coordination and Host–Guest Interactions. *J. Am. Chem. Soc* 2018, 140 (24), 7674–7680. [PubMed: 29856215]
- (16). Zhukhovitskiy AV; Zhong M; Keeler EG; Michaelis VK; Sun JEP; Hore MJA; Pochan DJ; Griffin RG; Willard AP; Johnson JA Highly branched and loop-rich gels via formation of metal–organic cages linked by polymers. *Nat. Chem* 2015, 8, 33. [PubMed: 26673262]
- (17). Yin G-Q; Wang H; Wang X-Q; Song B; Chen L-J; Wang L; Hao X-Q; Yang HB; Li X Self-assembly of emissive supramolecular rosettes with increasing complexity using multitopic terpyridine ligands. *Nat. Commun* 2018, 9 (1), 567. [PubMed: 29422628]

- (18). Wang P; Moorefield CN; Jeong K-U; Hwang S-H; Li S; Cheng SZD; Newkome GR Dendrimer–Metallomacrocyclic Composites: Nanofiber Formation by Multi-Ion Pairing. *Adv. Mater* 2008, 20 (7), 1381–1385.
- (19). Kishimura A; Yamashita T; Aida T Phosphorescent Organogels via “Metallophilic” Interactions for Reversible RGB–Color Switching. *J. Am. Chem. Soc* 2005, 127 (1), 179–183. [PubMed: 15631467]
- (20). He Y; Bian Z; Kang C; Gao L Self-discriminating and hierarchical assembly of racemic binaphthyl-bisbipyridines and silver ions: from metallocycles to gel nanofibers. *Chem. Commun* 2011, 47 (5), 1589–1591.
- (21). Foster JA; Parker RM; Belenguer AM; Kishi N; Sutton S; Abell C; Nitschke JR Differentially Addressable Cavities within Metal–Organic Cage–Cross-Linked Polymeric Hydrogels. *J. Am. Chem. Soc* 2015, 137 (30), 9722–9729. [PubMed: 26153733]
- (22). di Gregorio MC; Ranjan P; Houben L; Shimon LJW; Rechav K; Lahav M; van der Boom ME Metal–Coordination-Induced Fusion Creates Hollow Crystalline Molecular Superstructures. *J. Am. Chem. Soc* 2018, 140 (29), 9132–9139. [PubMed: 29939733]
- (23). Li Z-Y; Xu L; Wang C-H; Zhao X-L; Yang H-B Novel platinum–acetylide metallocycles constructed via a stepwise fragment coupling approach and their aggregation behaviour. *Chem. Commun* 2013, 49 (55), 6194–6196.
- (24). Zhao G-Z; Chen L-J; Wang W; Zhang J; Yang G; Wang D-X; Yu Y; Yang H-B Stimuli-Responsive Supramolecular Gels through Hierarchical Self-Assembly of Discrete Rhomboidal Metallocycles. *Chem. Eur. J* 2013, 19 (31), 10094–10100. [PubMed: 23843226]
- (25). Zhang M; Li S; Yan X; Zhou Z; Saha ML; Wang Y-C; Stang PJ Fluorescent metallocycle-cored polymers via covalent linkage and their use as contrast agents for cell imaging. *Proc. Natl. Acad. Sci* 2016, 113 (40), 11100–11105. [PubMed: 27647900]
- (26). Yan X; Jiang B; Cook TR; Zhang Y; Li J; Yu Y; Huang F; Yang H-B; Stang PJ Dendronized Organoplatinum(II) Metallocyclic Polymers Constructed by Hierarchical Coordination-Driven Self-Assembly and Hydrogen-Bonding Interfaces. *J. Am. Chem. Soc* 2013, 135 (45), 16813–16816. [PubMed: 24187961]
- (27). Sun Y; Yao Y; Wang H; Fu W; Chen C; Saha ML; Zhang M; Datta S; Zhou Z; Yu H; Li X; Stang PJ Self-Assembly of Metallocages into Multidimensional Suprastructures with Tunable Emissions. *J. Am. Chem. Soc* 2018 140 (40), 12819–12828. [PubMed: 30212221]
- (28). Yu GC; Ye Y; Tong ZZ; Yang J; Li ZT; Hua B; Shao L; Li SJ A Porphyrin-Based Discrete Tetragonal Prismatic Cage: Host–Guest Complexation and Its Application in Tuning Liquid-Crystalline Behavior. *Macromol. Rapid Commun* 2016, 37 (18), 1540–1547. [PubMed: 27465623]
- (29). Zheng W; Yang G; Shao N; Chen L-J; Ou B; Jiang S-T; Chen G; Yang H-B CO₂ Stimuli-Responsive, Injectable Block Copolymer Hydrogels Cross-Linked by Discrete Organoplatinum(II) Metallocycles via Stepwise Post-Assembly Polymerization. *J. Am. Chem. Soc* 2017, 139 (39), 13811–13820. [PubMed: 28885839]
- (30). Zheng W; Chen L-J; Yang G; Sun B; Wang X; Jiang B; Yin G-Q; Zhang L; Li X; Liu M; Chen G; Yang H-B Construction of Smart Supramolecular Polymeric Hydrogels Cross-linked by Discrete Organoplatinum(II) Metallocycles via Post-Assembly Polymerization. *J. Am. Chem. Soc* 2016, 138 (14), 4927–4937. [PubMed: 27011050]
- (31). Chen L-J; Ren Y-Y; Wu N-W; Sun B; Ma J-Q; Zhang L; Tan H; Liu M; Li X; Yang H-B Hierarchical Self-Assembly of Discrete Organoplatinum(II) Metallocycles with Polysaccharide via Electrostatic Interactions and Their Application for Heparin Detection. *J. Am. Chem. Soc* 2015, 137 (36), 11725–11735. [PubMed: 26322626]
- (32). Wu N-W; Chen L-J; Wang C; Ren YY; Li X; Xu L; Yang H-B Hierarchical self-assembly of a discrete hexagonal metallocycle into the ordered nanofibers and stimuli-responsive supramolecular gels. *Chem. Commun* 2014, 50 (32), 4231–4233.
- (33). Chen L-J; Zhao G-Z; Jiang B; Sun B; Wang M; Xu L; He J; Abliz Z; Tan H; Li X; Yang H-B Smart Stimuli-Responsive Spherical Nanostructures Constructed from Supramolecular Metallodendrimers via Hierarchical Self-Assembly. *J. Am. Chem. Soc* 2014, 136 (16), 5993–6001. [PubMed: 24684256]

- (34). Zheng W; Yang G; Jiang S-T; Shao N; Yin G-Q; Xu L; Li X; Chen G; Yang H-B A tetraphenylethylene (TPE)-based supra-amphiphilic organoplatinum(ii) metallacycle and its self-assembly behaviour. *Mater. Chem. Front* 2017, 1 (9), 1823–1828.
- (35). Xu X-D; Yao C-J; Chen L-J; Yin G-Q; Zhong Y-W; Yang H-B Facile Construction of Structurally Defined Porous Membranes from Supramolecular Hexakistriphenylamine Metallacycles through Electropolymerization. *Chem. Eur. J* 2016, 22 (15), 5211–5218. [PubMed: 26771048]
- (36). Ren Y-Y; Xu Z; Li G; Huang J; Fan X; Xu L Hierarchical self-assembly of a fluorescence emission-enhanced organogelator and its multiple stimuli-responsive behaviors. *Dalton Trans* 2017, 46 (2), 333–337. [PubMed: 27921100]
- (37). Zhou Z; Yan X; Cook TR; Saha ML; Stang PJ Engineering Functionalization in a Supramolecular Polymer: Hierarchical Self-Organization of Triply Orthogonal Non-covalent Interactions on a Supramolecular Coordination Complex Platform. *J. Am. Chem. Soc* 2016, 138 (3), 806–809. [PubMed: 26761393]
- (38). Yan X; Cook TR; Pollock JB; Wei P; Zhang Y; Yu Y; Huang F; Stang PJ Responsive Supramolecular Polymer Metallogel Constructed by Orthogonal Coordination-Driven Self-Assembly and Host/Guest Interactions. *J. Am. Chem. Soc* 2014, 136 (12), 4460–4463. [PubMed: 24621148]
- (39). Tian Y; Yan X; Saha ML; Niu Z; Stang PJ Hierarchical Self-Assembly of Responsive Organoplatinum(II) Metallacycle–TMV Complexes with Turn-On Fluorescence. *J. Am. Chem. Soc* 2016, 138 (37), 12033–12036. [PubMed: 27608138]
- (40). Cao L; Wang P; Miao X; Dong Y; Wang H; Duan H; Yu Y; Li X; Stang PJ Diamondoid Supramolecular Coordination Frameworks from Discrete Adamantanoid Platinum(II) Cages. *J. Am. Chem. Soc* 2018, 140 (22), 7005–7011. [PubMed: 29746782]
- (41). Yan X; Li S; Pollock JB; Cook TR; Chen J; Zhang Y; Ji X; Yu Y; Huang F; Stang PJ Supramolecular polymers with tunable topologies via hierarchical coordination-driven self-assembly and hydrogen bonding interfaces. *Proc. Natl. Acad. Sci* 2013, 110 (39), 15585–15590. [PubMed: 24019475]
- (42). Zhang J; Marega R; Chen L-J; Wu NW; Xu X-D; Muddiman DC; Bonifazi D; Yang H-B Hierarchical Self-Assembly of Supramolecular Hydrophobic Metallacycles into Ordered Nanostructures. *Chem. Asian J* 2014, 9 (10), 2928–2936. [PubMed: 25139814]
- (43). Jiang B; Zhang J; Zheng W; Chen L-J; Yin G-Q; Wang Y-X; Sun B; Li X; Yang H-B Construction of Alkynylplatinum(II) Bzimp-Functionalized Metallacycles and Their Hierarchical Self-Assembly Behavior in Solution Promoted by Pt···Pt and π – π Interactions. *Chem. Eur. J* 2016, 22 (41), 14664–14671. [PubMed: 27533298]
- (44). Yin G; Chen L; Wang C; Yang H Fabrication of Neutral Supramolecular Polymeric Films via Post-electropolymerization of Discrete Metallacycles. *Chin. J. Chem* 2018, 36 (2), 134–138.
- (45). Wang Y; Gu Y; Keeler EG; Park JV; Griffin RG; Johnson JA Star PolyMOCs with Diverse Structures, Dynamics, and Functions by Three-Component Assembly. *Angew. Chem. Int. Ed* 2017, 56 (1), 188–192.
- (46). Uchida J; Yoshio M; Sato S; Yokoyama H; Fujita M; Kato T Self-Assembly of Giant Spherical Liquid-Crystalline Complexes and Formation of Nanostructured Dynamic Gels that Exhibit Self-Healing Properties. *Angew. Chem. Int. Ed* 2017, 56 (45), 14085–14089.
- (47). Kuritani M; Tashiro S; Shionoya M Organic and Organometallic Nanofibers Formed by Supramolecular Assembly of Diamond-Shaped Macrocyclic Ligands and PdII Complexes. *Chem. Asian J* 2013, 8 (7), 1368–1371. [PubMed: 23554351]
- (48). Liu Y; Shi B; Wang H; Shangguan L; Li Z; Zhang M; Huang F Construction of Metallacycle-Cored Supramolecular Gel by Hierarchical Self-Assembly of Metal Coordination and Pillar[5]arene-Based Host–Guest Recognition. *Macromol. Rapid Commun* 2018, 1800655.
- (49). Chan Y-T; Moorefield CN; Soler M; Newkome GR Unexpected Isolation of a Pentameric Metallomacrocyclic from the FeII-Mediated Complexation of 120° Juxtaposed 2,2':6',2''-Terpyridine Ligands. *Chem. Eur. J* 2010, 16 (6), 1768–1771. [PubMed: 20066709]
- (50). Piot M; Abecassis B; Brouri D; Troufflard C; Proust A; Izzet G Control of the hierarchical self-assembly of polyoxometalate-based metallomacrocyclics by redox trigger and solvent composition. *Proc. Natl. Acad. Sci. USA* 2018, 115 (36), 8895–8900. [PubMed: 30131428]

**Scheme 1.**

The combination of ditopic and tritopic building blocks results in 2-dimensional convex polygons and 3-dimensional polygons, which in turn generate soft material.

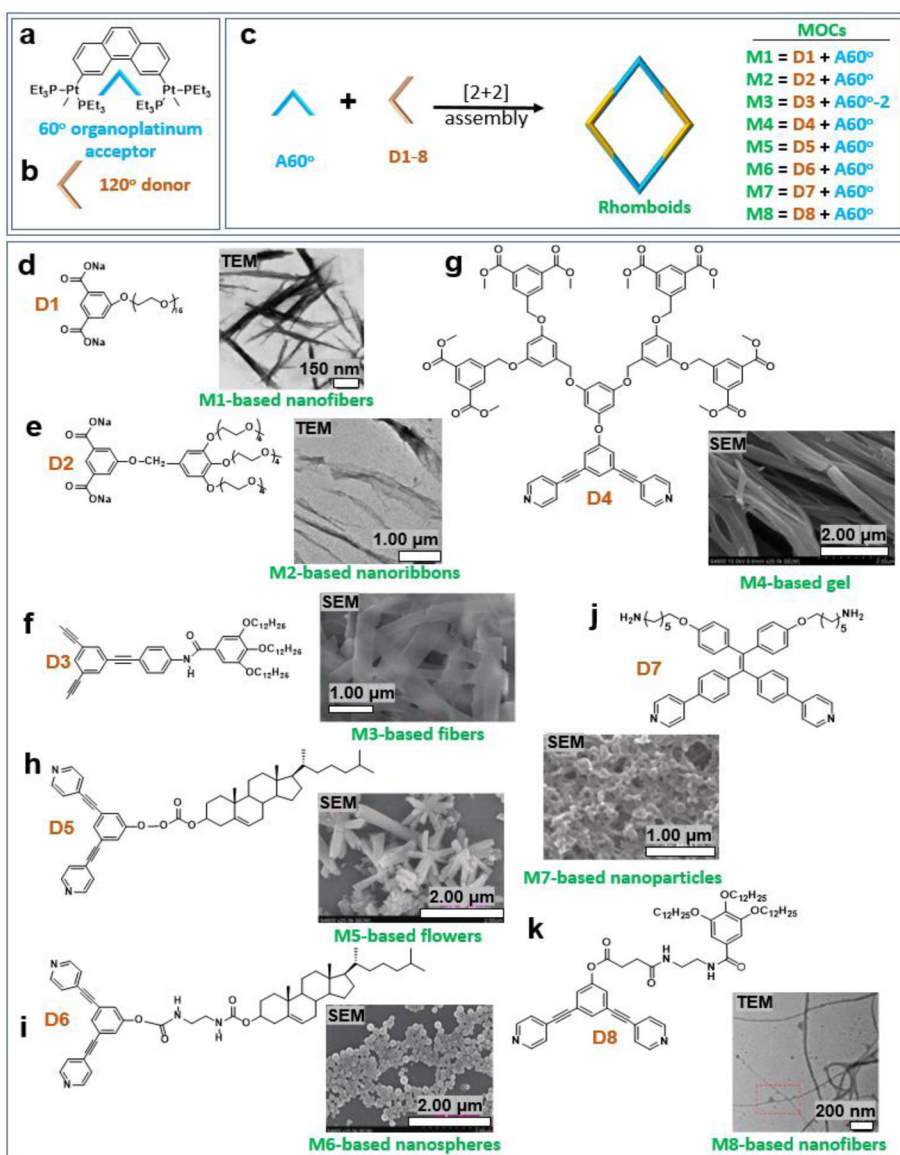


Figure 1. (a–k) 60° organoplatinum (II) acceptor-based rhomboids and the resultant soft suprastructures. Adapted with permission from ref 7, 14, 23–26. Copyright 2013 American Chemical Society, 2013 and 2016 the Royal Society of Chemistry, 2013 Wiley-VCH, 2016 National Academy of Sciences (USA).

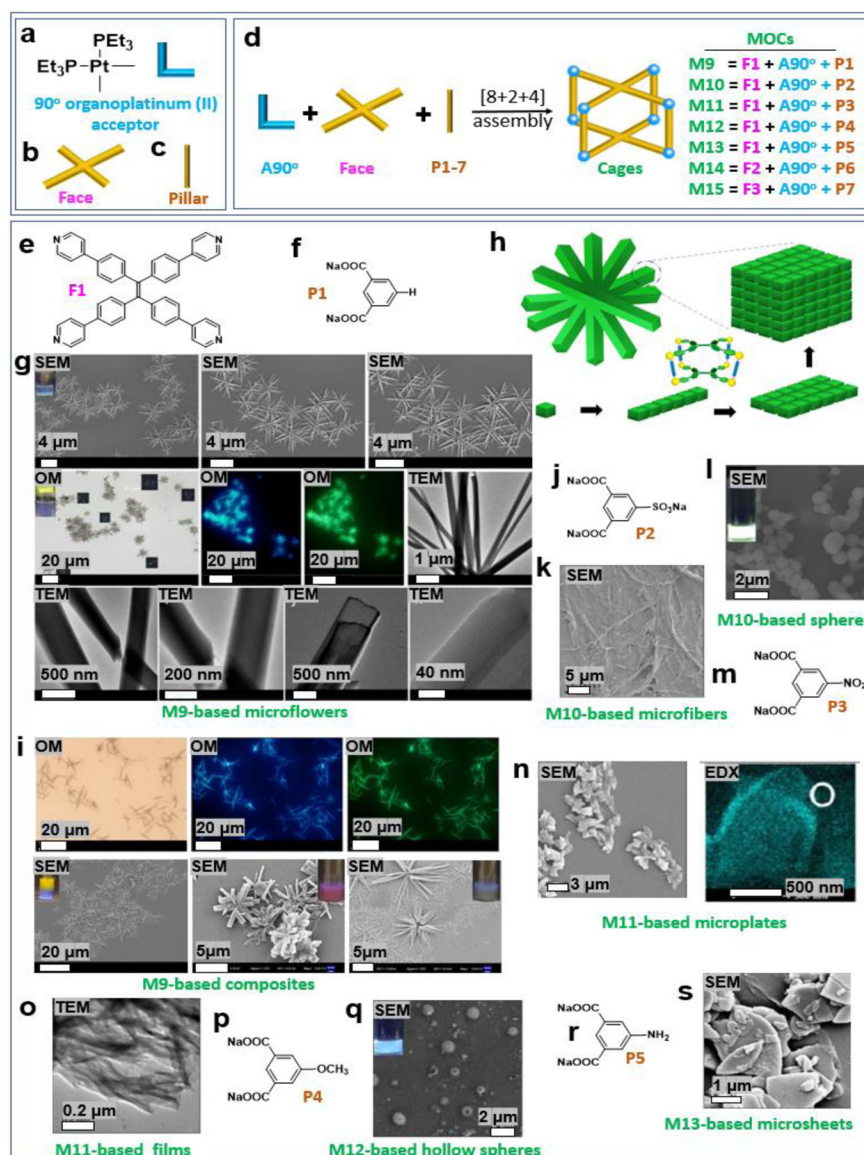


Figure 2. (a–s) 90° organoplatinum (II) acceptor-based metallacages and the resultant soft materials. Adapted with permission from ref 12, 27. Copyright 2018 American Chemical Society.

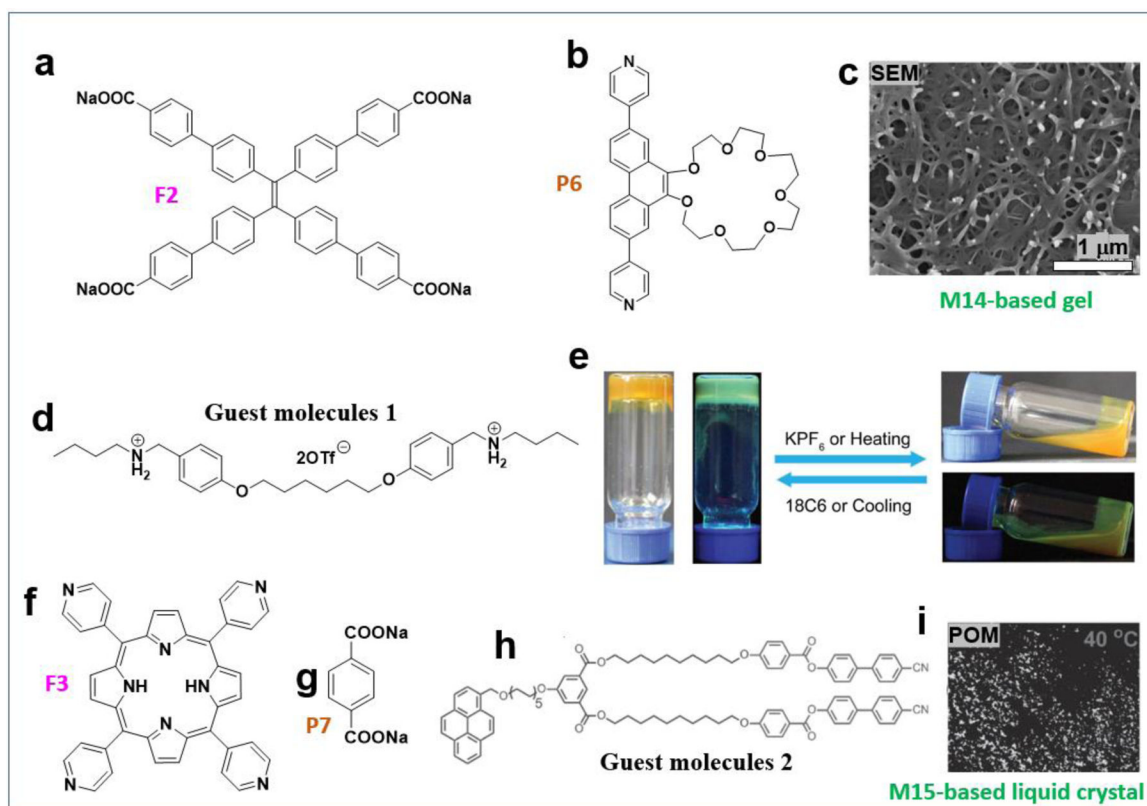


Figure 3. (a–h) 90° organoplatinum(II) acceptor-based MOFs and the resultant supramolecular polymers and liquid crystals. Adapted with permission from ref 15, 28. Copyright 2018 American Chemical Society, 2016 Wiley-VCH.

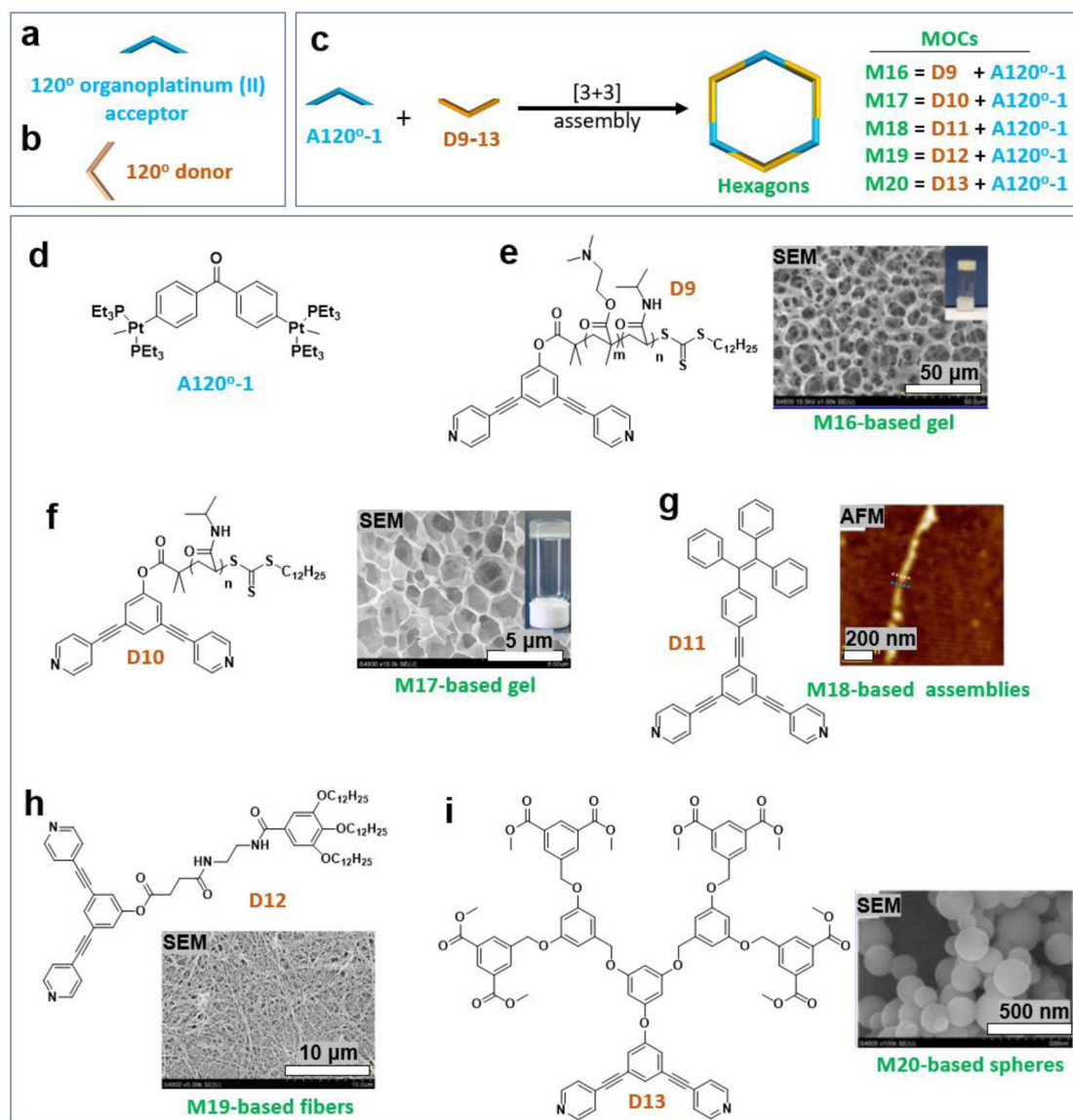


Figure 4. (a–i) 120° organoplatinum (II) acceptor-based MOCs and the resultant soft materials. Adapted with permission from ref 29–33. Copyright 2014–2017 American Chemical Society, 2014 the Royal Society of Chemistry.

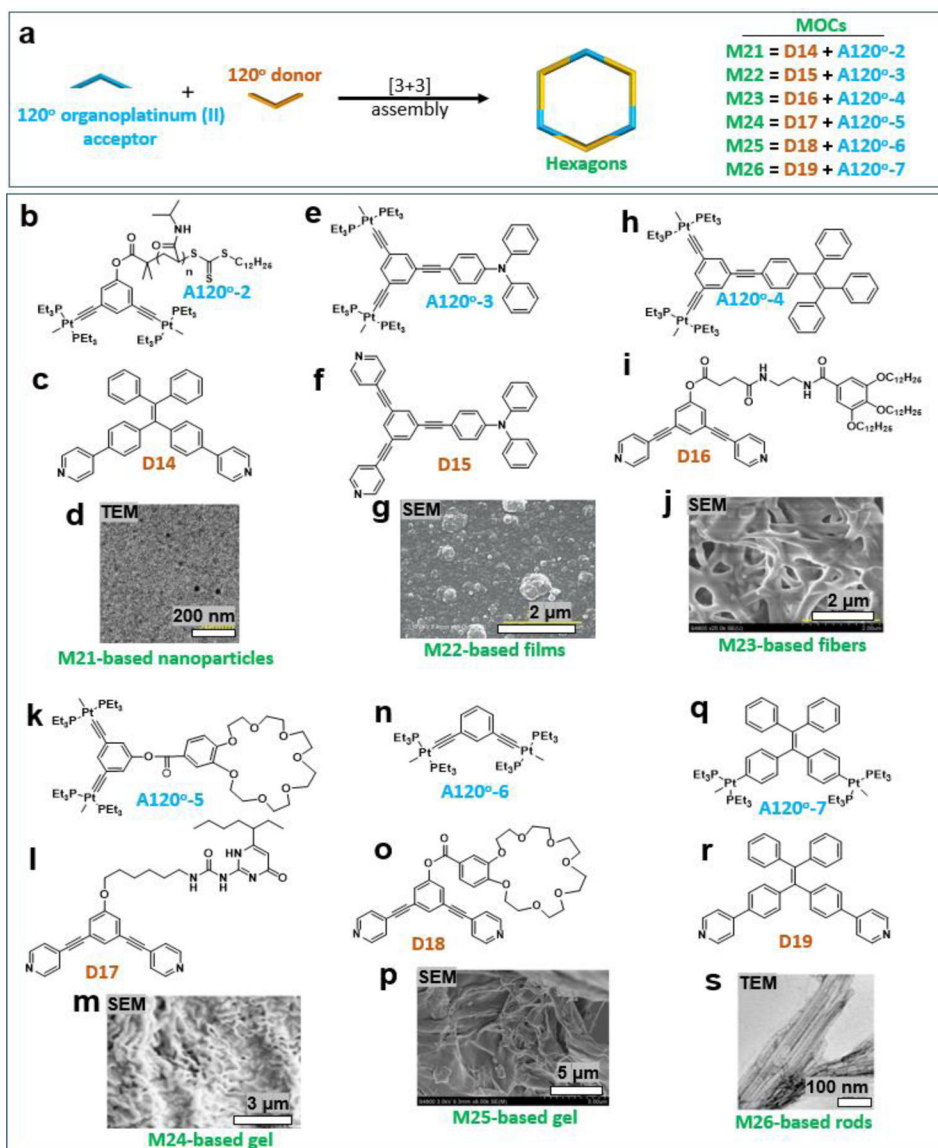


Figure 5.
 (a–s) 120° organoplatinum (II) acceptor-based MOCs and the resultant soft materials.
 Adapted with permission from ref 34–39. Copyright 2017 the Royal Society of Chemistry,
 2016 Wiley-VCH, 2014 and 2016 American Chemical Society.

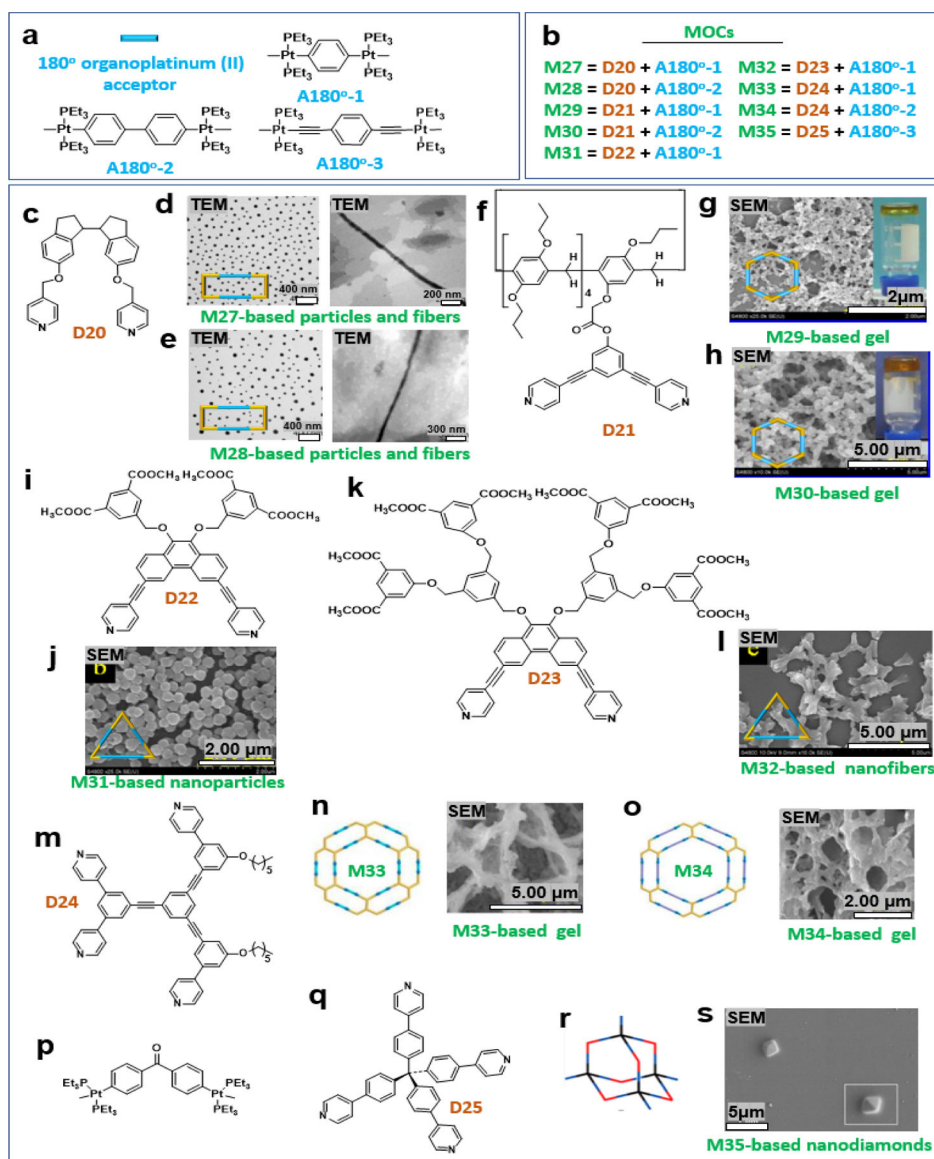


Figure 6. (a–s) 180° organoplatinum (II) acceptor-based MOCs and the resultant soft materials. Adapted with permission from ref 8–11, 40. Copyright 2016 Elsevier, 2014 National Academy of Sciences (USA), 2014–2015 and 2018 American Chemical Society.

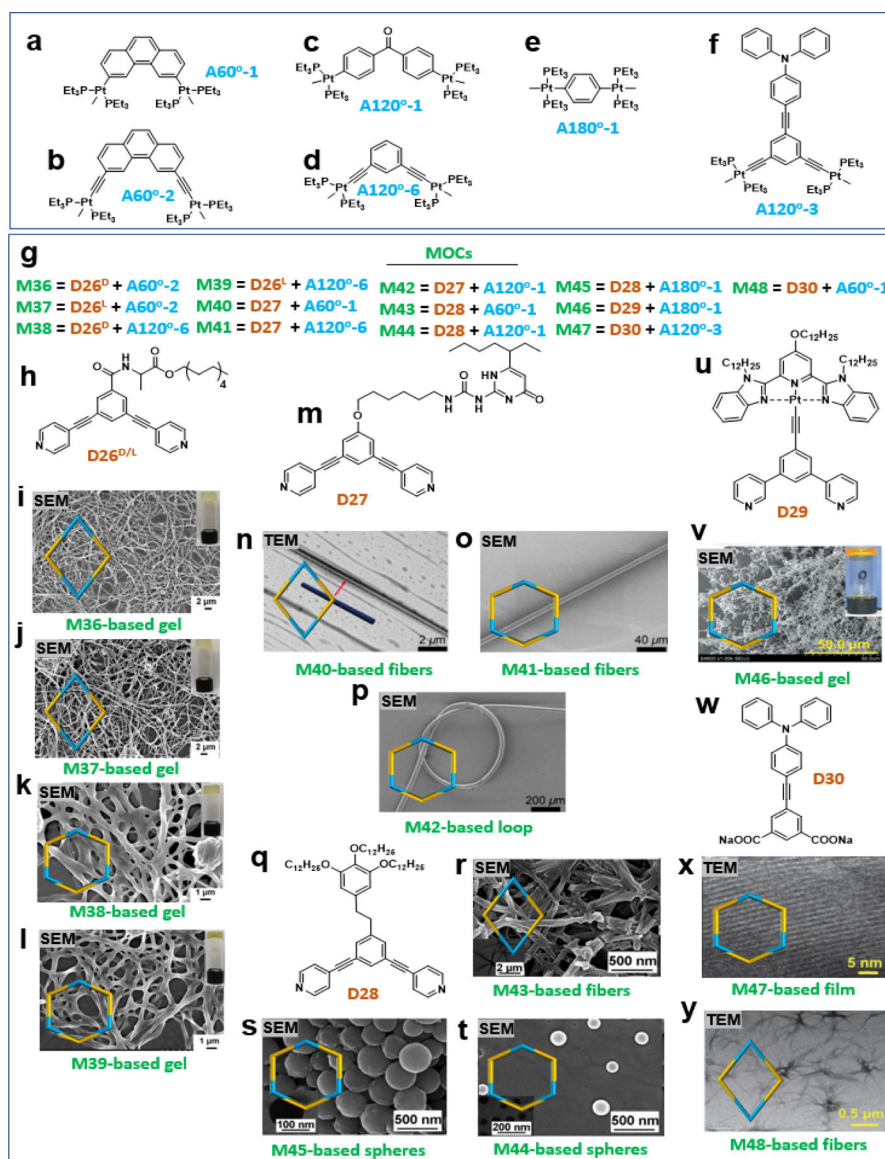


Figure 7. (a–y) 180° organoplatinum (II) acceptor-based MOCs and the resultant soft materials. Adapted with permission from ref 13, 41–44. Copyright 2018 American Chemical Society, 2013 National Academy of Sciences (USA), 2014, 2016 and 2018 Wiley-VCH.

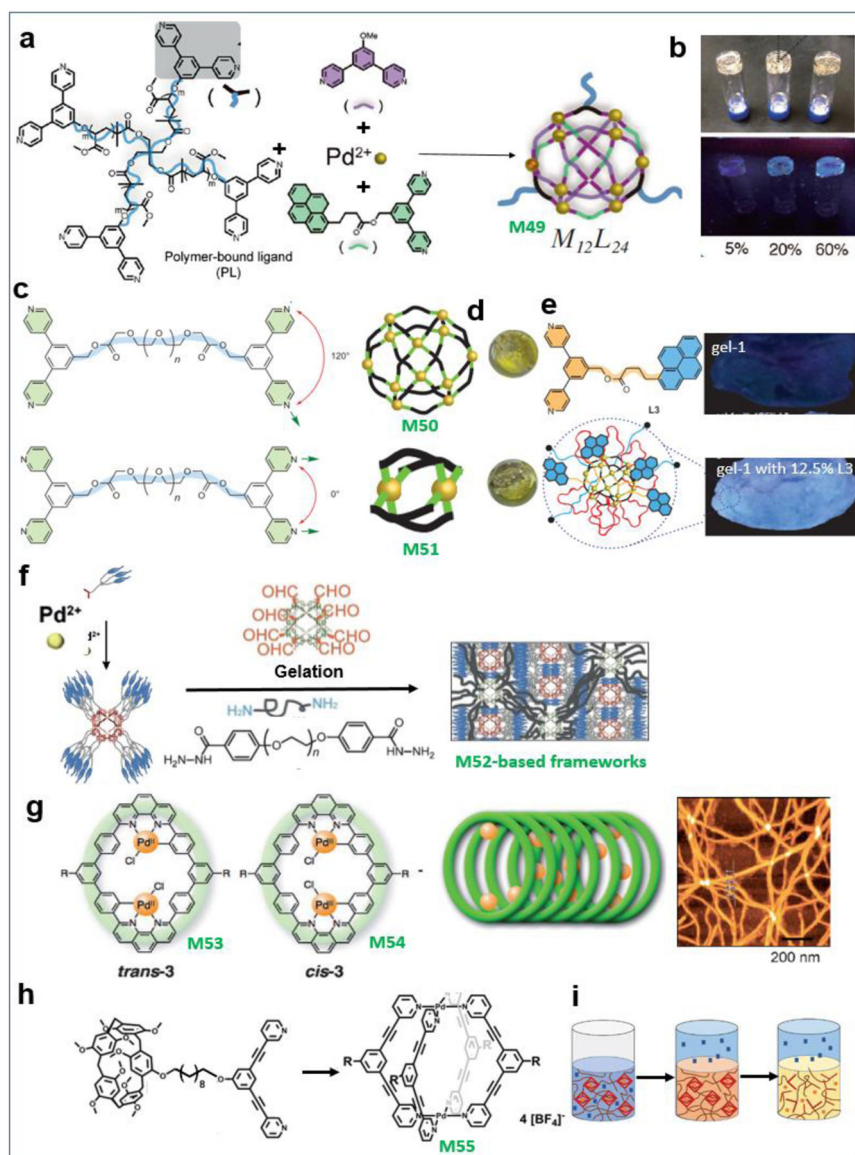


Figure 8. Palladium-based MOFs and the resultant soft suprastructures. (a–i) **M49–55**. Adapted with permission from ref 16, 45–48. Copyright 2015 Nature Publishing Group, 2013 and 2017–2018 Wiley-VCH.

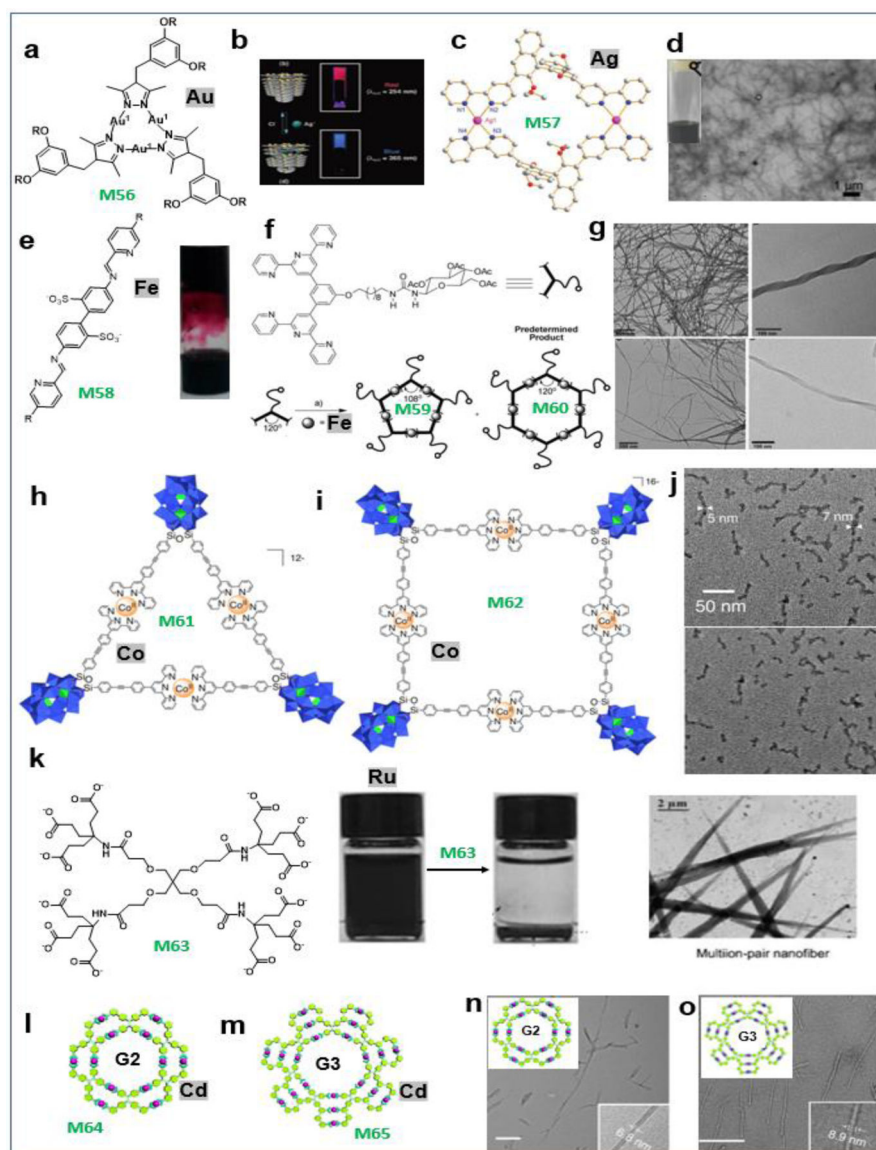
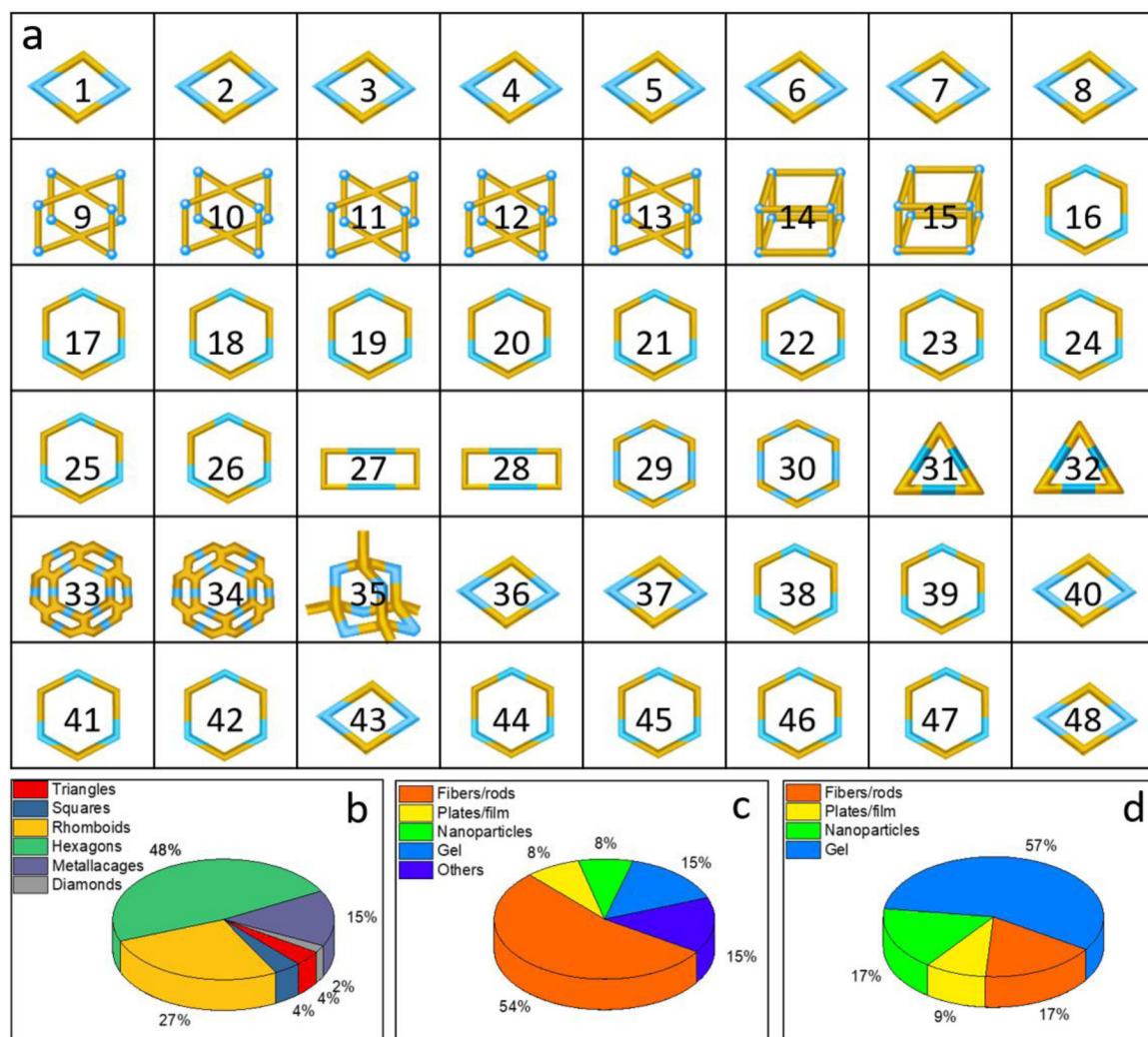


Figure 9. Palladium-based MOFs and the resultant soft suprastructures. (a–o) **M56–65**. Adapted with permission from ref 17–19, 21, 49, 50. Copyright 2018 Nature Publishing Group, 2008 and 2010–2011 Wiley-VCH, 2005 and 2015 American Chemical Society, 2018 National Academy of Sciences (USA).

**Figure 10.**

(a) MOC for higher-order assembly (MOC 1–48); (b) pie chart of various MOCs for constructing soft material; (c) rhomboid MOCs based soft materials; (d) hexagon MOCs based soft materials.